Fracture 1977, Volume 2, ICF4, Waterloo, Canada, June 19 - 24, 1977

OBSERVATIONS ON THE EFFECT OF CEMENTITE PARTICLES ON THE FRACTURE OF SPHEROIDIZED CARBON STEELS

S. P. Rawal[1] and J. Gurland[2]

INTRODUCTION

The influence of temperature and microstructure on the fracture toughness of spheroidized carbon steels is partially due to a transition in the mode of fracture in front of a macroscopic crack tip from ductile rupture to cleavage as the temperature is decreased and as the carbon content or carbide particle size are increased [1]. It is the purpose of this paper to relate a number of observations on crack initiation and propagation to the Ritchie, Knott and Rice criterion for unstable cleavage fracture [2].

EXPERIMENTAL PROCEDURES

The carbon content of the steels ranges from 0.13 to 1.46%. Yield strength and fracture toughness were determined at -198°, -170°, -150° and -110°C. The fracture toughness parameter K_{IC} was evaluated under plane strain conditions by using circumferentially notched and fatigue-cracked cylindrical specimens. The characteristics of the fracture surfaces and the microstructural parameters were determined by optical and electron microscopy. Details of the experimental procedures are provided in reference 3.

EXPERIMENTAL RESULTS

1. *Association of Cleavage Cracks with Particles.* The preferential location of cleavage crack initiation and propagation at cementite particles is well established [4], and it was confirmed once more by the observation of arrested crack segments in unnotched tensile specimens fractured at low temperature. It was shown by quantitative metallography that the number of particles in contact with the fracture path, per unit length, is greater than the number of particles intercepted per unit length of random test lines and that the number of broken particles per unit length of fracture path increases with decreasing length of the crack segments (Figure 1), suggesting that crack initiation does indeed occur at the particles.

2. *Fracture Surface Characteristics.* Observation of the fracture surfaces and of the fracture surface profiles reveal two different modes of fracture in the region near the crack tip. At -196°C and -170°C, the specimens generally fracture in a brittle manner. The fracture surfaces exhibit facets, river markings, and tongues characteristic of cleavage fracture; also cleavage crack initiation sites at particles are often observed near the fatigue crack border.

---

1. Now with New England Metals Co., Providence, Rhode Island, U. S. A.
2. Division of Engineering, Brown University, Providence, Rhode Island, U. S. A.

At -150°C, in the tougher specimens, and at 110°C in all specimens one notices a stretch zone and dimples indicating fibrous, i.e., ductile fracture in a region between the fatigue crack area and the final brittle fracture. Carbide particles are seen in a few of the dimples. The fatigue crack is appreciably blunted in the low carbon steels (0.13%C) after fracture at -110°C.

3. *Crack Tip Blunting.* The events occurring at the fatigue crack tip in a low carbon steel (0.13%) at -110°C are shown in detail in Figure 2, which shows a notched, fatigue-cracked specimen unloaded just before fracture. The figure reveals extensive plastic deformation in the grains ahead of the crack tip, also broken particles and voids; all indications strongly support the ductile nature of the crack initiation process in this alloy at this temperature.

4. *Fracture Toughness.* The fracture toughness is plotted in Figure 3 as a function of $\sigma_y^{1/2} f^{-1/6}$ (dotted line, cleavage fracture initiation) or $\sigma_y^{1/2} f^{-1/4}$ (solid line, ductile rupture initiation), where σ_y is the yield strength of the steels and f is the volume fraction of cementite. The functional dependence of K_{IC} on volume fraction is derived [5] from an approximate failure criterion proposed by Rice and Johnson [6]:

$$K_{IC} = [2E\Delta\sigma_y]^{1/2} \qquad (1)$$

where Δ is the interparticle spacing, and E is the Young's modulus. We find good agreement with equation (1) if Δ is taken as the planar nearest neighbour particle spacing ($0.36\ df^{-1/2}$) for specimens undergoing ductile initiation, and if Δ is taken as the volume nearest neighbour particle spacing ($0.45\ df^{-1/3}$) for cleavage initiated fracture specimens [1]. In general, the fracture toughness increases with increasing temperature, and decreasing volume fraction and decreasing size of the carbide particles.

DISCUSSION

a) *Stress Condition.* The work of Rice and Johnson [6] and the finite element solutions of Levy et al [7] and Rice and Tracey [8] for the elastic-perfectly plastic crack tip stress state provide the stress distribution ahead of the crack tip, with the maximum stress occurring at a distance of approximately twice the crack opening displacement (COD), and the maximum stress value is approximately equal to $3\sigma_y$. According to the literature, a stress of 203-242 ksi (1400-1668 MN/m^2) is sufficient to form voids at the particle matrix interface [9] and a stress of approximately 215 ksi (1482 MN/m^2) can cause particle fracture [10]. Comparison of the stress required for particle fracture or decohesion with the measured yield strength values indicates that the maximum stress intensity ($3\sigma_y$) reaches the particle or interface strength in almost all specimens; the exception being three specimens at -110°C which have $3\sigma_y$ values less than 1300 MN/m^2. The stress conditions for particle or interface cracking therefore exist within a few grains or particle spacings from the crack tip in most of our specimens and, indeed, broken particles or interfacial voids are often observed in this region.

b) *Cleavage Crack Propagation.* Assuming that the fracture processes near the crack tip are initiated by particle cracking or interface decohesion, the next step is to consider the conditions of growth of the microscopic cracks. The conditions for slip induced cleavage crack propagation are given by the Ritchie, Knott, and Rice (RKR) model [2] which requires

that the principal stress, σ_{yy}, at the crack tip equals or exceeds a critical cleavage stress, σ_f^*, over a microstructurally significant size scale, X_o. The value of σ_f^* is generally calculated from rigid-plastic solutions for notched bars in bending [2, 10]. It was equated by RKR [2] to the critical tensile stress causing unstable cleavage crack propagation from microscopic crack nuclei. The latter is given by Smith [11] as the fracture propagation stress of a crack nucleated within a grain boundary carbide particle, which, in the absence of dislocation contributions, is given by:

$$\sigma_f^* = \left[\frac{4E\gamma_f}{\pi(1-\eta^2)\bar{d}}\right]^{1/2} \qquad (2)$$

where γ_f is the effective surface energy of ferrite, η is the Poisson's ratio and $\bar{d}$ is the mean carbide thickness. This stress is taken as being essentially independent of temperature. Neglect of the dislocation contribution accounts for an error of only 1-2% in the calculated values of σ_f^* for the steels under consideration.

The procedures of the RKR model have been applied to the data of this investigation using equation 2 to calculate the fracture stress σ_f^*, with $\gamma_f = 14\ J/m^2$, and determining the stress intensification σ_{yy}/σ_o ahead of the crack tip from the plastic-elastic stress distribution for small scale yielding conditions given in RKR [2] graphically as a function of the dimensionless parameter $X_o/(K/\sigma_o)^2$ for various hardening exponents, where σ_{yy} is the longitudinal tensile stress ahead of a crack; σ_o is the yield stress; X_o is the distance from the crack tip within which σ_{yy} is equal to or larger than σ_{yy} at X_o (except for the very near tip region), and K is the stress intensity factor. The strain hardening exponent n was taken to be 0.2. An average value of X_o was obtained by matching the experimental K_{IC} value of each specimen with the RKR procedure, using $\sigma_{yy} = \sigma_f^*$, and solving for X_o. In that case, we obtain $X_{average} = 1.3\lambda_G$, when λ_G is the ferrite grain size. The values of K_{IC} calculated by the RKR procedure, with $X_o = 1.3\lambda_G$, are compared with the observed values of K_{IC} in Figure 4, for all specimens broken at -196°, -170° and -150°C in which fracture propagation by cleavage was observed near the fatigue-crack tip. Also, for the same specimens, the values of the ratio σ_f^*/σ_y range from 1.6 to 3.86 with most values below 3. The fracture process suggested by these results is one of cleavage crack propagation from particle-associated cracks in a region where the stress concentration is sufficient to reach the critical crack propagation stress value, i.e., where $\sigma_{yy} > \sigma_f^*$.

One may speculate about the length of X_o in terms of the grain size, λ_G, by referring back to Smith's model for the growth of slip induced grain boundary carbide cracks [11]. The model assumes that a grain boundary particle is fractured by the impingement of a slip band or dislocation pile-up proportional in length to the grain size, and that the stress concentration at the tip of the pile-up will contribute to the propagation of the microcrack. The critical event, however, may include the propagation of the crack through a grain boundary into a second grain, thereby requiring the highly stressed region to be larger than one grain.

At very low temperatures, when σ_f^* is of magnitude comparable to or smaller than the yield stress, the RKR criterion reduces to:

$$K_{IC} = \sigma_f^* \sqrt{2\pi X_o} \qquad (3)$$

At -196°C, the ratios of K_{IC}, measured, and $\sigma_f^*\sqrt{2\pi X_o}$, calculated, vary from 0.7 to 1.2, i.e., the measured and calculated terms are approximately equal, indicating linear elastic stress conditions at that temperature which justify the use of equation 3. With increasing temperatures, the stress distribution deviates more and more from the purely elastic case and both σ_f^*/σ_y and $K_{IC}/\sigma_f^*\sqrt{2\pi X_o}$ increase in magnitude (Figure 5), although cleavage crack propagation at the fatigue crack tip still occurs at -170°C and -150°C in those specimens with $\sigma_f^*/\sigma_y \leq 3.86$ and K_{IC} obtainable by the RKR procedure.

c) *Fibrous Rupture Initiation and Propagation.* The specimens at the upper end of the plot of Figure 5 are not included in the group defined by the preceding criterion of cleavage fracture. For all specimens broken at -110°C, and for the tougher specimens at -150°C, the cleavage fracture stress appreciably exceeds the available stress intensification, i.e., $\sigma_f^*/\sigma_y > 3.86$, and the RKR criterion is no longer satisfied. Ductile rupture surface characteristics are generally observed in these specimens in the region between the fatigue crack tip and the final brittle fracture. The failure in this region occurs by cavity growth in the triaxial stress field ahead of the crack tip [1].

As mentioned previously, the calculated stress levels ahead of the fatigue-crack tip are sufficient to break the particles in almost all specimens even at -110°C, especially if the stress amplification includes strain hardening effects. At the same time, high strains are developed in this region which are compatible with both void initiation and void growth. The true strains at fracture at distances Δ_2 (planar nearest neighbour particle spacing) and Δ_3 (volume nearest neighbour particle spacing) from the crack tips were estimated by the method of Rice and Johnson [6], with strain values larger than 0.1 and 0.2, respectively, obtained in all specimens of ductile fracture character. Tanaka et al [12] calculated that a critical plastic strain of 0.05 is sufficient for cavity formation at particles larger than 0.4 - 0.5μ. Also, cavity growth in the triaxial stress field ahead of the crack tip by factors of 3.3 and 11 for true strains of 0.1 and 0.2, respectively, was calculated by Rice and Tracey [8]. Therefore, if the initial void size is taken as equal to the average particle size and the final void size is assumed to be of the order of magnitude of the planar nearest neighbour particle spacing Δ_2, the microstructute of these steels satisfies the geometrical condition for void coalescence to form a planar void sheet, with values of $\Delta_2/\bar{d}$ ranging from 1.7 to 6.2. The significance of the particle spacing Δ_2 is further supported by the good agreement between the experimental data and equation (1) if $\Delta = \Delta_2$ for the specimens undergoing fibrous initiation, (Figure 3).

It is surprising to note in Figure 3 that equation (1), with constant particle size, holds for the cleavage initiated fracture specimens at -196°C, -170°C, and -150°C, since its derivation is based on a model of ductile crack growth [5, 6]. Equation (1) may perhaps be justified in this case by stipulating that, for cleavage fracture, the nearest particle distance in a volume, Δ_3, be proportional to the distance of the maximum stress, $2\delta_t$, ahead of the fatigue crack tip. The extent of the region of large plastic deformation at the onset of crack extension (which is a distance approximately twice the critical crack opening displacement, δ_t) increases with temperature; δ_t being very approximately comparable to Δ_3 at -196°C, and to Δ_2 at -110°C.

ACKNOWLEDGEMENTS

This work was supported by the U. S. Energy Research and Development Administration (U. S. Atomic Energy Commission), under contract (11-1)3084. The authors thank Professor J. R. Rice for very helpful discussions, and the Army Mechanics and Materials Research Center, Watertown, Massachusetts for supplying the steels.

REFERENCES

1. RAWAL, S. P. and GURLAND, J., Proceedings of the 2nd Int. Conf. on Mechanical Behaviour of Materials, Boston, 1976, (to be published).
2. RITCHIE, R. O., KNOTT, J. F. and RICE, J. R., J. Mech. Phys. Solids, 21, 1973, 395.
3. RAWAL, S. P., Ph. D. Thesis, Brown University, June, 1975.
4. McMAHON, C. J. and COHEN, M., Acta Met., 13, 1965, 591-604.
5. HAHN, G. T. and ROSENFIELD, A. R., Met. Trans., 6A, 1975, 653-668.
6. RICE, J. R. and JOHNSON, M. A., "Inelastic Behaviour of Solids", M. F. Kanninen et al, Editors, McGraw-Hill, New York, 1970, 641.
7. LEVY, N., MARCAL, P. V., OSTERGREN, W. J. and RICE, J. R., Int. J. Fracture Mechanics, 7, 1971, 143.
8. RICE, J. R. and TRACEY, D. M., "Computational Fracture Mechanics", in Numerical and Computational Methods in Structural Mechanics, S. J. Fenves et al, Editors, Academic Press, New York, 1973.
9. ARGON, A. S. and IM, J., Met. Trans., 6A, 1975, 839.
10. GRIFFITHS, J. R. and OWEN, D. R. I., J. Mech. Phys. Solids, 19, 419.
11. SMITH, E., Int. J. Fracture Mechanics, 4, 1968, 131.
12. TANAKA, K., MORI, T. and NAKAMURA, T., Phil. Mag., 21, 1970, 267.

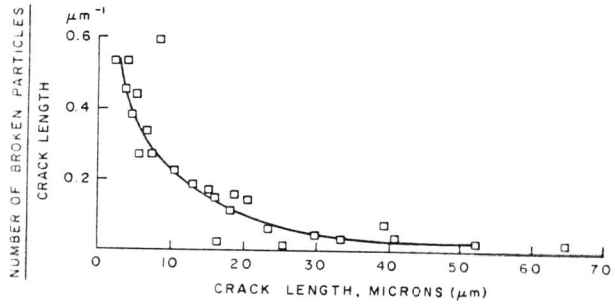

Figure 1 Plot of the Number of Broken Particles per unit Crack Length versus Crack Segment Length

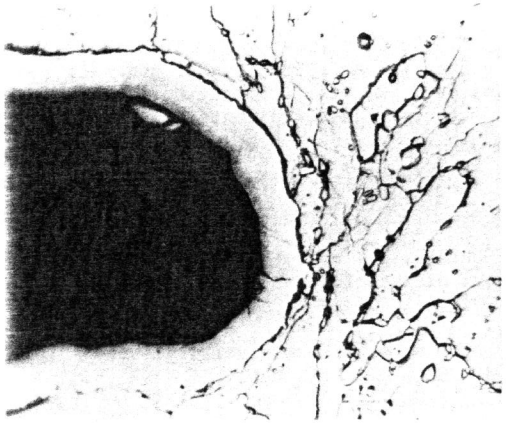

Figure 2 Micrograph Showing Broken Particles and Voids Ahead of the Blunted Crack Tip. Nickel Plated - Approximate Magnification 900X

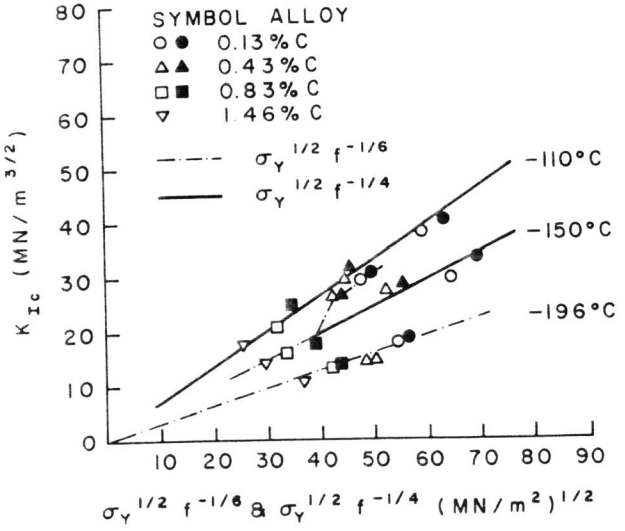

Figure 3 Influence of the Volume Fraction of Carbide Particles and Yield Strength on the Plain Strain Fracture Toughness

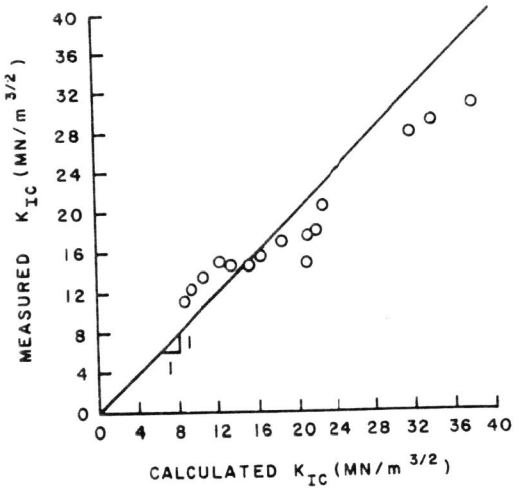

Figure 4 Comparison of Measured K_{IC} and Calculated K_{IC}, with $X = 1.3\lambda_G$ and Small Scale Yielding Conditions

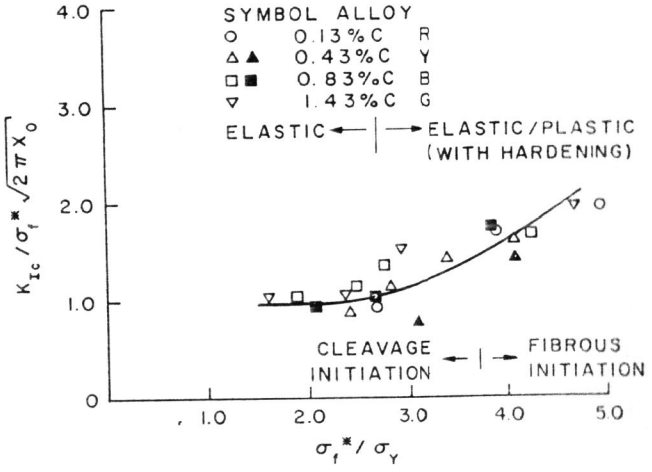

Figure 5 Plot of $K_{IC}/\sigma_f^*\sqrt{2\pi X_o}$ vs. σ_f^*/σ_y